metals

MDPI

Article

Novel Confinement Possibility for Laser Shock: Use of Flexible Polymer Confinement at 1064 nm Wavelength

Corentin Le Bras [1,2,*], Alexandre Rondepierre [1,3], Mohammad Ayad [1], Yann Rouchausse [1], Matthieu Gervais [1,*], Stéphane Valadon [2] and Laurent Berthe [1,*]

[1] Laboratoire PIMM, UMR 8006, ENSAM, CNRS, CNAM, HESAM, 151 boulevard de l'Hôpital, 75013 Paris, France; alexandre.rondepierre@fr.thalesgroup.com (A.R.); Mohammad.ayad@ensam.eu (M.A.); yann.rouchausse@ensam.eu (Y.R.)
[2] Airbus Operation S.A.S, 316 route de Bayonne-B.P. D4101, CEDEX 9, 31060 Toulouse, France; stephane.valadon@airbus.com
[3] Thales Las France, 78990 Elancourt, France
* Correspondence: corentin.le_bras@ensam.eu (C.L.B.); matthieu.gervais@lecnam.net (M.G.); laurent.berthe@ensam.eu (L.B.); Tel.: +33-171-936-533 (C.L.B.)

Abstract: Through the years, laser shock peening became a treatment of choice in the aerospace industry to prolong the life of certain critical pieces. Water flow is commonly used as a confinement to improve the process capability but some applications cannot allow for water presence in the area of interest. In a previous article, an alternative to the water confinement was presented, a flexible polymer confinement was used and demonstrated the production of pressures equivalent to the water configuration treatment. However, laser parameters have been restricted to a wavelength in the visible range at 532 nm. In this paper, the study is extended to 1064 nm which is commonly used in LSP applications and with two different pulse durations. A 1064 nm near infra-red laser is used to do pressure characterization of shots with polymer confinement through Velocity Interferometer System for Any Reflector (VISAR) measurements coupled with Finite Element Modelling on Abaqus software. The results show that the pressures produced by the confinement is slightly lower with the 1064 nm wavelength, similar to what is observed with the classic water confined regime when switching from 532 nm to a near infra-red wavelength. Nevertheless, the high level of pressure produced by laser shock under the polymer confinement configuration allows for the treatment of common types of metal alloys used in the aerospace industry. Although the use of such a confinement has yet to be applicable to peening setups, it has already uses in some single shot configurations such as LasAT where it allows the avoidance of the water flow optimization.

Keywords: laser shock peening; polymers; polymer confinement; VISAR measurement; finite element method

Citation: Le Bras, C.; Rondepierre, A.; Ayad, M.; Rouchausse, Y.; Gervais, M.; Valadon, S.; Berthe, L. Novel Confinement Possibility for Laser Shock: Use of Flexible Polymer Confinement at 1064 nm Wavelength. *Metals* **2021**, *11*, 1467. https://doi.org/10.3390/met11091467

Academic Editors: Yuji Sano and Nikolai Kashaev

Received: 13 July 2021
Accepted: 9 September 2021
Published: 16 September 2021

1. Introduction

The study of pulsed laser technology, leading to the development of laser shock peening traces back to the 1960s with the work of Askar et al. [1]. The technique took off after Anderholm found out that using a transparent overlay on the shocked surface could greatly improve the capability of the process by producing higher pressures and applying them two times longer [2]. The use of laser shock peening then became more and more prevalent as time passed [3].

Today, laser shock peening is commonly used in the aerospace industry to prolong the life of specific pieces, hence prolonging the life of plane fleets. Laser shock peening presents many advantages when compared with classical peening, making it a solution of interest. First, it is a non-contact method and the use of laser allows for a good control over the overlapping of the shots as well as the pressure loading induced. Moreover, the pieces treated exhibit a better fatigue life behavior compared to the ones treated with conventional

peening [4]. Corrosion resistance as well as crack initiation and propagation resistance are also gained through the treatment [5,6]. The residual stresses imparted in the pieces and leading to the improved fatigue life behavior are induced deeper in the matter compared to conventional peening, affecting depths up to 1.5 mm when classic peening goes up to around 300 µm in the case of aluminium alloys [7].

In an industrial setting, treatments are realized in confined regime. Usually, this type of configuration uses a thin water layer on top of the target to treat. During shock, the water confinement layer blocks the plasma expansion in the air. This leads to the production of higher pressures that are also applied two times longer than without any confinement. In the case of certain specific pieces, water cannot fulfill the role of the confinement. An alternative is needed to fill this type of applications. Other confinements have been briefly studied in laboratory setting but consisted mainly in quartz crystals or solid transparent materials for the demonstration of the shock impedance mismatch theory [8]. We proposed in a previous article to use a flexible adhesive polymer confinement instead of water [9]. The material demonstrated a pressure production under laser irradiation equivalent to the ones obtained using water. However, all the experiments of this study were realized on a 532 nm green laser as opposed to the lasers commonly used for LSP treatment on materials which typically are 1064 nm near infra-red lasers. In this paper, we present new results obtained with a polymer confinement with a 1064 nm laser using the same pressure measurement approach to allow for a comparison between the behavior of the polymer under the two wavelengths.

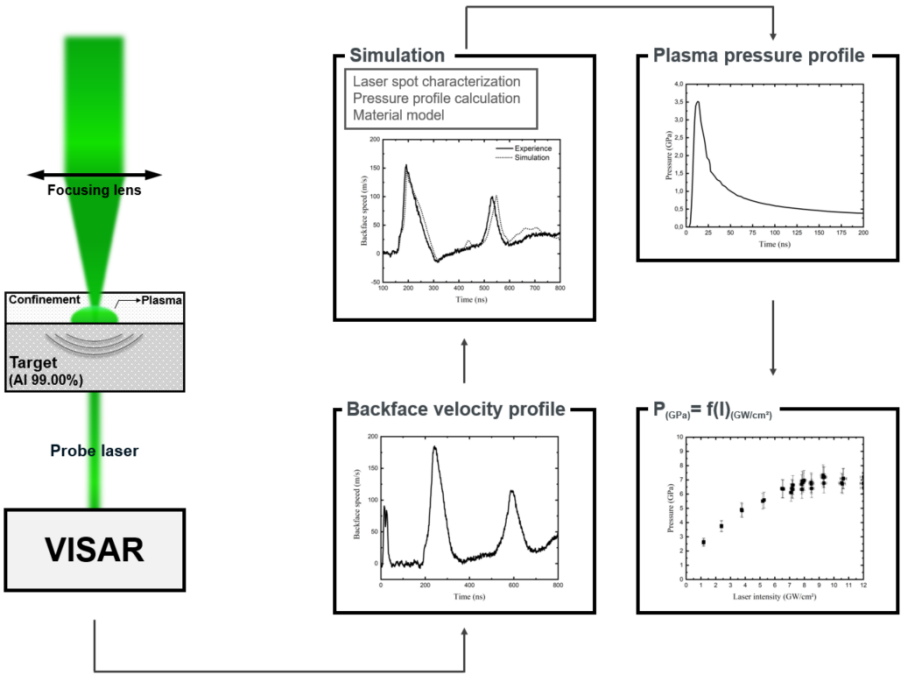

Figure 1. Setup used to calculate pressure from the backface velocity measurements.

2. Materials and Methods

The experimental path used to obtain the pressure produced is extensively described in [9]. It is described in figure 1. A VISAR is used to measure the velocity profile of the rear free surface of aluminium targets irradiated by laser on their front surface. The maximum pressure of each shot is determined by reproducing the velocity profiles with a FEM simulation on Abaqus software through the use of the Johnson-Cook model [10]. The value obtained for each laser shot is then correlated with the laser intensity of said shots. This method is in the continuation of the one developed in works by Peyre [11]. Further work by Amarchinta demonstrated the accuracy of the Johnshon-Cook model over

the elastic perfectly plastic and the Zerilli–Armstrong models [12]. Moreover the use of a pressure profile more representative of the experimental one allows for a more accurate modelling of the process.

2.1. Material

The polymer confinement chosen is an acrylate based polymer tape with a thickness of 1 mm. More information on this material choice can be found in [9]. The targets selected for the pressure determination were pure 0.5 mm thick aluminium foils (99.0%, AL000645, Goodfellow) cut to a $\approx 15 \times 15$ mm size. Aluminium was chosen for its well known properties. The thickness chosen allows a large enough delay between peaks of the velocity profiles which represent the shockwave going back and forth in the material. The contact between the confinement and the target was ensured by the adhesive properties of the polymer. Multiple single spot experiments were performed for each laser intensity tested to ensure the reproducibility of the results.

2.2. Laser

Laser pulses are generated with the THEIA Nd:YAG diode-pumped solid-state laser from Thales (Elancourt, France) working at 1064 nm wavelength. The energy delivered can go up to 1 J with a Gaussian pulse showing a Full Width at Half Maximum (FWHM) duration tunable from 7 to 21 ns and a repetition rate of 200 Hz. The laser spot diameters used for the experiments are 0.7 and 1.2 mm. A Diffractive Optical Element (DOE) was used to homogenize the beam energy distribution [13,14]. The laser intensities used ranged from 1.4 to 10.9 GW/cm². The pulse spatial profile was measured with a Camera Basler acA2040-25gm/ gc, Monochrome, CMOS 1" with a pixel size of 5.5 × 5.5 µm. Figure 2 shows the experimental laser spot of 1.2 mm used.

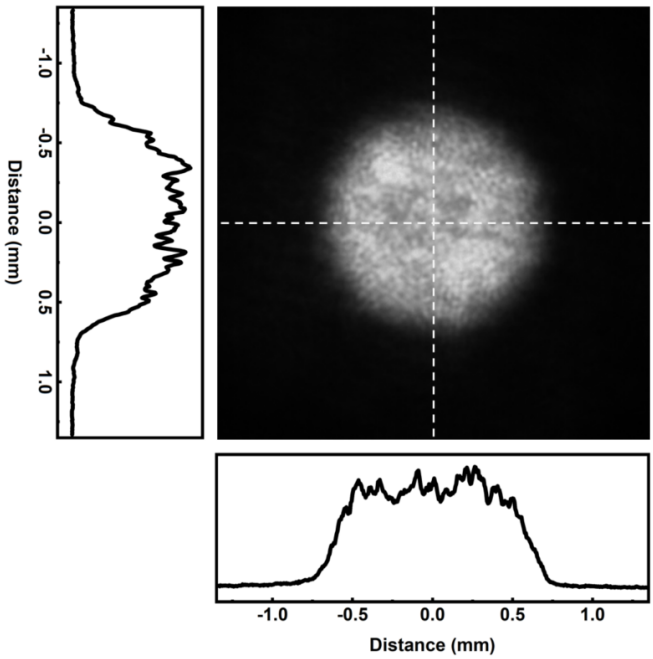

Figure 2. Laser spot profile obtained from camera measurement for a 1.2 mm laser spot with a DOE.

2.3. Transmission Measurements

The transmission of the polymer confinement has been assessed by using a calorimeter (QE50LP-H-MB-QED, Gentec) to measure the energy of a laser pulse with and without the confinements on the laser path. The water transmission was evaluated for a 1 mm layer from the database [15].

2.4. VISAR

The backface velocity profiles of the shots realized on the aluminium targets were measured with a VISAR [16,17]. It is a non-contact diagnostic based on a Michelson interferometer measuring the Doppler shift in wavelength of a target put into motion by a shockwave. In this case, the Doppler shift of the rear free surface of an aluminium target is measured. The VISAR used is composed of two parts: an interferometer making the signal interfere with itself and a probe continuous laser (532 nm, 5W, Coherent) focused on the center of the incident laser pulse, sending the Doppler shift information from the target to the interferometer.

2.5. FEM Simulation

Finite Element Modelling simulations of the backface velocity profiles obtained by VISAR measurements were realised on Abaqus software. A 2D axisymmetric explicit model was used. To take into account the high strain rates involved in the LSP process, a Johnson-Cook material model was chosen [18].

2.5.1. Target Geometry and Boundary Conditions

The target used for the FEM simulation was modelled as a rectangle with a length of 10 mm and a thickness of 500 µm, considering the axisymmetric axis. The elements chosen were CAX4R elements (Continuum, 4-nodes bilinear axisymmetric, quadrilateral, reduced integration, hourglass control). The mesh was refined in the area of interest with an element size of 1 µm × 1 µm while the rest of the area was meshed using a BIAS function in the direction normal to the impact making the elements bigger as they were further away from the shocked area. One node at the bottom surface away from the shocked area was fixed as a boundary condition to represent the sample holder effect on the target.

2.5.2. Constitutive Material's Model

Shocks produced by nanosecond laser pulses demonstrate high strain rate (around 10^6 to 10^7 s^{-1}) [19]. To accurately represent this type of interaction, the Johnson-Cook constitutive model was chosen. This model defines the Von Mises yield criterion as follow:

$$\sigma = (\sigma_y + K\epsilon_p^n)\left(1 + Cln\left(\frac{\dot{\epsilon}}{\dot{\epsilon_0}}\right)\right)\left(1 - \left(\frac{T - T_0}{T_{melt} - T_0}\right)^m\right). \quad (1)$$

With σ_y the yield stress, B the hardening modulus ϵ_p the equivalent plastic deformation, n the hardening coefficient, C the strain rate sensitivity parameter, $\dot{\epsilon}$ the strain rate during the process, $\dot{\epsilon_0}$ the strain rate at $t = 0$, T_{melt} the fusion temperature, T_0 the room temperature, m a thermal softening coefficient, E the Young's modulus and ν the Poisson's ratio. Since the thermal part has no significant influence on the simulation of the process [20] it is neglected. The Johnson-Cook parameters used for the FEM simulation are given in Table 1.

Table 1. Parameters used for the Johnson-Cook material model with an aluminum target (99.0%) [21].

Material	σ_y (GPa)	B (GPa)	n	C	$\dot{\epsilon_0}$	E (GPa)	ν
Aluminum	0.129	0.2	0.45	0.03	0.01	69	0.33

2.5.3. Spatial and temporal pressure profiles

The temporal pressure profiles $P = f(x, y, t)$ where generated using a VDOLAD subroutine. The $P(t)$ profile generated was adjusted to provide coherence between the experimental and numerical results by slightly playing on the rising edge and release time. The intensity profile of the laser spot was obtained through camera imaging of the laser spot used. The maximum intensity in the laser spot profile can be correlated to the maximum pressure areas of the spot [22,23].

3. Results and Discussion

3.1. Transmission

Transmission results for water and polymer tape are given in Table 2. Measurements on the 1 mm polymer tape result in a 95% transmission of the incident laser energy, similar to what was obtained at 532 nm previously. Water, on the other hand was considered fully transparent at 532 nm and had a transmission of 95% at 1064 nm for a 1 mm layer.

Table 2. Optical transmission of water and polymer tape at 532 and 1064 nm.

Confinement	Transmission	
	532 nm	**1064 nm**
Water	100%	95%
Polymer tape	90%	95%

3.2. Pressure Measurement

Figure 3 shows the plasma pressure determined from backface velocity measurement depending on the incident laser intensity for pulse durations of 7 and 21 ns at 1064 nm wavelength. Pressures at 532 nm with water and solid confinement from [9] as well as pressures under water confined regime at 1053 nm with a 10 ns laser pulse from [24] are also reported. The pressure increases linearly for the two wavelengths up to 6 GW/cm^2. It goes from 1.8 GPa at 0.8 GW/cm^2 to 5.3 GPa at 6 GW/cm^2. For near infra-red shots, going higher than 6 GW/cm^2 causes the pressure to saturate due to the triggering of the breakdown phenomenon in the confinement as previously explained in [9] while with the shots at 532 nm the breakdown starts at 7 GW/cm^2 allowing the process to reach higher pressures. At an intensity threshold, a breakdown plasma occurs at the surface of the confinement. It absorbs the incident energy of the laser pulse and, as a result, limits the amount of energy effectively brought to the surface of the confined target surface.

Overall, the shots in the near infra-red wavelengths produce lower pressures than the one at 532 nm independently of the confining medium chosen. However, in the near infra-red configuration, the water confined regime produces higher pressures than the flexible polymer confinement, reaching 4.9 GPa at 5 GW/cm^2 while the solid confinement reaches 4.2 GPa at 5.1 GW/cm^2. A possible explanation would be that the polymer confinement is more prone to the presence of impurities or porosities due to its structure and adhesive nature, causing more loss in the incident laser energy.

The polymer confinement demonstrates lower pressures at 1064 nm than at 532 nm. The pressure is around 30% lower at 2.6 GW/cm^2 and the gap is slowly reduced with increasing laser intensities ($-$18% at 6.2 GW/cm^2 and $-$14% at 7.1 GW/cm^2. The water confined regime demonstrated the same trend with pressures in the near infra-red being around 30% lower at 1.1 GW/cm^2 and then reducing the gap at $-$15% at 2.4 GW/cm^2 and finally $-$5% at 5.2 GW/cm^2. The decreasing of the pressure gap between the two wavelength is faster in the water confined regime than with the flexible confinement experiments. The difference can be explained by the damaging of the confinement which causes the absorption of more incident laser energy during the shots as well as triggers the breakdown phenomenon sooner. These data were compared with the pressures obtained while using the code given in Scius-Bertrand et al. work [24] and gave similar results.

Table 3 gathers power density thresholds at which the pressure starts to saturate ($I_{P_{sat}}$) and the corresponding maximum pressures associated (P_{max}) as a function of the wavelength and pulse duration. The different pulse durations tested also showed the shift to a lower $I_{P_{sat}}$ threshold and by extension lower P_{sat} when longer pulse durations were used. At 1064 nm, the maximum pressure reaches 7 GPa at 10.9 GW/cm^2 for a 7 ns pulse against 5.1 GPa at 7.8 GW/cm^2 for a 21 ns pulse. This trend is in agreement with current breakdown description [25] and previous pressure measurements in water [26]: laser energy absorption is conducted by inverse Bremsstrahlung phenomenon which implies a

wavelength dependency: shorter wavelength are more absorbed thus explaining the lower pressures observed at 1064 nm.

These results demonstrate the capability of a polymer confinement to be used in multiple settings as well as its versatility. Due to its stable transmission and its good adhesive properties it can easily be adapted to different setups or lasers, giving a glimpse of potential possibilities for laser shock peening of all types of metals from low to high elastic limit ones. The comparison with results obtained in water confined regime shows an equivalent pressure production in both wavelengths presented. These results comfort the place of a flexible polymer confinement along side water for specific applications in the aeronautical industry but also for other applications such as for LasAT experiments in which case it allows for the avoidance of the water flow calibration. The similarity of the results shows that the phenomena taking place during the laser interaction with water and flexible polymer confinement are likely akin in terms of laser-matter interaction.

Table 3. Maximum pressure produced and breakdown thresholds of the polymer confinement for 532 and 1064 nm lasers for the different laser pulse duration used.

Wavelength (nm)	Confinement	Pulse duration (ns)	Threshold ($I_{P_{sat}}$) (GW/cm²)	Maximum Pressure (P_{max}) (GPa)
532	Polymer	9	7	7.4
1064	Polymer	7	7	7
1064	Polymer	21	6	5.1
1053	Water	10	6	5.3
532	Water	9	7	7

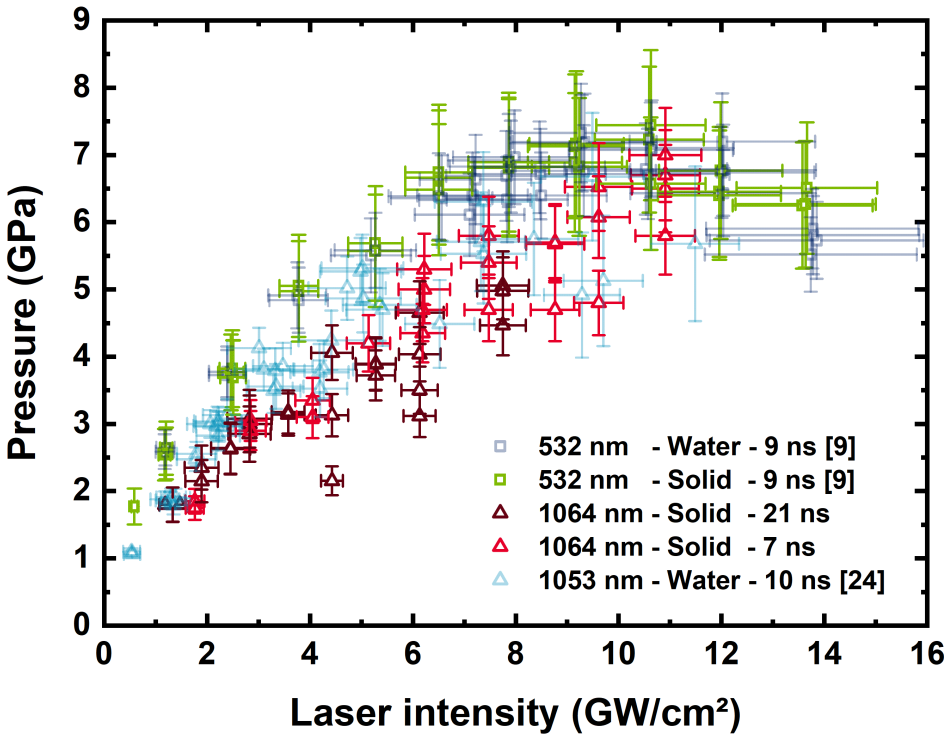

Figure 3. Pressure measurements obtained from VISAR measurements with the polymer confinement at 1064 nm for a 7 and 21 ns laser pulse. Results are compared with pressures obtained in [9] at 532 nm with a pulse duration of 9 ns and with results at 1053 nm with a pulse duration of 10 ns from [24].

4. Conclusions

Pressure measurements on laser shocks were realised by coupling VISAR experiments with FEM simulations on Abaqus. The modelling of the backface velocity profiles obtained allowed the extraction of the front face pressure produced by the laser shock. The laser intensities used ranged from 1.3 to 10.9 GW/cm^2 with two pulse durations, respectively 7 and 21 ns. These results complete the one already obtained during a previous study on flexible polymer confinement under a 532 nm illumination. The 1064 nm wavelength chosen in this work is closer to the one of the commonly used lasers for material reinforcement through laser shock peening. The pressure obtained, although it is a little lower than with a 532 nm laser pulse, is high enough to allow the treatment of all types of metal alloys used in the aerospace industry and achieve good mechanical properties, thus paving the way to potential new options of peening.

As of now, the biggest hurdle of the process is to tackle the damaging of the polymer tape in between shots. Consequently, the next steps of the work will focus on a way to use the polymer confinement with repeated shots for area treatment as well as understanding the different phenomena at work during shock to further the comprehension of the polymer damaging under laser shock. An alternative solution being worked on is to automate the placing and replacement of the confinement to avoid any damaging problem between shots.

Author Contributions: Data curation, A.R.; Formal analysis, C.L.B. and M.A.; Investigation, A.R. and L.B.; Methodology, C.L.B., A.R., M.A. and L.B.; Project administration, M.G., S.V. and L.B.; Resources, Y.R.; Supervision, S.V. and L.B.; Validation, L.B.; Writing—original draft, C.L.B.; Writing—review & editing, C.L.B., A.R., M.A., M.G., S.V. and L.B. All authors have read and agreed to the published version of the manuscript.

Funding: Airbus company, CNRS, ANR Forge laser (ANR-18-CE08-0026).

Acknowledgments: The authors would like to thanks CEA for lending its VISAR for the experiments realised.

Conflicts of Interest: The authors declare no conflict of interest.

Reference

1. Askar'yan, G.A.; Moroz, E.M. Pressure on Evaporation of Matter in a Radiation Beam. *Sov. J. Exp. Theor. Phys.* **1963**, *16*, 1638.
2. Anderholm, N. Laser-generated stress waves. *Appl. Phys. Lett.* **1970**, *16*, 113–115. [CrossRef]
3. Clauer, A.H. Laser Shock Peening, the Path to Production. *Metals* **2019**, *9*, 626. [CrossRef]
4. Sanchez, A.; You, C.; Leering, M.; Glaser, D.; Furfari, D.; Fitzpatrick, M.; Wharton, J.; Reed, P. Effects of laser shock peening on the mechanisms of fatigue short crack initiation and propagation of AA7075-T651. *Int. J. Fatigue* **2021**, *143*, 106025. [CrossRef]
5. Pavan, M.; Furfari, D.; Ahmad, B.; Gharghouri, M.; Fitzpatrick, M. Fatigue crack growth in a laser shock peened residual stress field. *Int. J. Fatigue* **2019**, *123*, 157–167. [CrossRef]
6. Sun, R.; Li, L.; Guo, W.; Peng, P.; Zhai, T.; Che, Z.; Li, B.; Guo, C.; Zhu, Y. Laser shock peening induced fatigue crack retardation in Ti-17 titanium alloy. *Mater. Sci. Eng. A* **2018**, *737*, 94–104. [CrossRef]
7. Peyre, P.; Fabbro, R. Laser shock processing: a review of the physics and applications. *Opt. Quantum Electron.* **1995**, *27*, 1213–1229.
8. Hong, X.; Wang, S.; Guo, D.; Wu, H.; Wang, J.; Dai, Y.; Xia, X.; Xie, Y. Confining medium and absorptive overlay: Their effects on a laser-induced shock wave. *Opt. Lasers Eng.* **1998**, *29*, 447–455. [CrossRef]
9. Le Bras, C.; Rondepierre, A.; Seddik, R.; Scius-Bertrand, M.; Rouchausse, Y.; Videau, L.; Fayolle, B.; Gervais, M.; Morin, L.; Valadon, S.; et al. Laser shock peening: Toward the use of pliable solid polymers for confinement. *Metals* **2019**, *9*, 793. [CrossRef]
10. Smith, M. *ABAQUS/Standard User's Manual, Version 6.9*; Simulia: Johnston, RI, USA, 2009.
11. Peyre, P.; Chaieb, I.; Braham, C. FEM calculation of residual stresses induced by laser shock processing in stainless steels. *Model. Simul. Mater. Sci. Eng.* **2007**, *15*, 205. [CrossRef]
12. Amarchinta, H.; Grandhi, R.; Langer, K.; Stargel, D. Material model validation for laser shock peening process simulation. *Model. Simul. Mater. Sci. Eng.* **2008**, *17*, 015010. [CrossRef]
13. Bardy, S.; Aubert, B.; Berthe, L.; Combis, P.; Hébert, D.; Lescoute, E.; Rullier, J.L.; Videau, L. Numerical study of laser ablation on aluminum for shock-wave applications: Development of a suitable model by comparison with recent experiments. *Opt. Eng.* **2016**, *56*, 011014. [CrossRef]
14. Ünaldi, S.; Papadopoulos, K.; Rondepierre, A.; Rouchausse, Y.; Karanika, A.; Deliane, F.; Tserpes, K.; Floros, G.; Richaud, E.; Berthe, L. Towards selective laser paint stripping using shock waves produced by laser-plasma interaction for aeronautical applications on AA 2024 based substrates. *Opt. Laser Technol.* **2021**, *141*, 107095. [CrossRef]

15. Polyanskiy, M.N. Refractive Index Database. 2014. Available online: https://github.com/polyanskiy/refractiveindex.info-database (accessed on 13 July 2021)
16. Tollier, L.; Fabbro, R.; Bartnicki, E. Study of the laser-driven spallation process by the velocity interferometer system for any reflector interferometry technique. I. Laser-shock characterization. *J. Appl. Phys.* **1998**, *83*, 1224–1230. [CrossRef]
17. Tollier, L.; Fabbro, R. Study of the laser-driven spallation process by the VISAR interferometry technique. II. Experiment and simulation of the spallation process. *J. Appl. Phys.* **1998**, *83*, 1231–1237. [CrossRef]
18. Johnson, G.R. A constitutive model and data for materials subjected to large strains, high strain rates, and high temperatures. In Proceedings of the 7th International Symposium on Ballistics, Hague, The Netherlands, 19–21 April 1983; pp. 541–547.
19. Peyre, P.; Fabbro, R.; Merrien, P.; Lieurade, H. Laser shock processing of aluminium alloys. Application to high cycle fatigue behaviour. *Mater. Sci. Eng. A* **1996**, *210*, 102–113. [CrossRef]
20. Hfaiedh, N.; Peyre, P.; Song, H.; Popa, I.; Ji, V.; Vignal, V. Finite element analysis of laser shock peening of 2050-T8 aluminum alloy. *Int. J. Fatigue* **2015**, *70*, 480–489. [CrossRef]
21. Cuq-Lelandais, J.P. Etude du Comportement Dynamique de Matériaux Sous Choc Laser Subpicoseconde. Ph.D. Thesis, ISAE-ENSMA Ecole Nationale Supérieure de Mécanique et d'Aérotechique, Poitiers, France, 2010.
22. Berthe, L.; Fabbro, R.; Peyre, P.; Tollier, L.; Bartnicki, E. Shock waves from a water-confined laser-generated plasma. *J. Appl. Phys.* **1997**, *82*, 2826–2832. [CrossRef]
23. Peyre, P.; Berthe, L.; Scherpereel, X.; Fabbro, R.; Bartnicki, E. Experimental study of laser-driven shock waves in stainless steels. *J. Appl. Phys.* **1998**, *84*, 5985–5992. [CrossRef]
24. Scius-Bertrand, M.; Videau, L.; Rondepierre, A.; Lescoute, E.; Rouchausse, Y.; Kaufman, J.; Rostohar, D.; Brajer, J.; Berthe, L. Laser induced plasma characterization in direct and water confined regimes: New advances in experimental studies and numerical modelling. *J. Phys. D Appl. Phys.* **2020**, *54*, 055204. [CrossRef]
25. Peyre, P.; Fabbro, R.; Berthe, L.; Dubouchet, C. Laser shock processing of materials, physical processes involved and examples of applications. *J. Laser Appl.* **1996**, *8*, 135–141. [CrossRef]
26. Berthe, L.; Fabbro, R.; Peyre, P.; Bartnicki, E. Wavelength dependent of laser shock-wave generation in the water-confinement regime. *J. Appl. Phys.* **1999**, *85*, 7552–7555. [CrossRef]